

Long non-coding RNA-AK138945 regulates myocardial ischemia-reperfusion injury via the miR-1-GRP94 signaling pathway

Yanying Wang^{1#}, Jian Huang^{2#}, Han Sun^{1#}, Jie Liu¹, Yingchun Shao^{1,4}, Manyu Gong^{1,5}, Xuewen Yang¹, Dongping Liu¹, Zhuo Wang³, Haodong Li¹, Yanwei Zhang¹, Xiyang Zhang¹, Zhiyuan Du¹, Xiaoping Leng^{3*}, Lei Jiao^{1*}, Ying Zhang^{1*}

Abstract

Objective: Myocardial ischemia-reperfusion injury (MIRI) is one of the leading causes of death from cardiovascular disease in humans, especially in individuals exposed to cold environments. Long non-coding RNAs (lncRNAs) regulate MIRI through multiple mechanisms. This study explored the regulatory effect of lncRNA-AK138945 on myocardial ischemia-reperfusion injury and its mechanism. **Methods:** *In vivo*, 8- to 12-week-old C57BL/6 male mice underwent ligation of the left anterior descending coronary artery for 50 minutes followed by reperfusion for 48 hours. *In vitro*, the primary cultured neonatal mouse ventricular cardiomyocytes (NMVCs) were treated with 100 $\mu\text{mol/L}$ hydrogen peroxide (H_2O_2). The knockdown of lncRNA-AK138945 was evaluated to detect cardiomyocyte apoptosis, and a glucose-regulated, endoplasmic reticulum stress-related protein 94 (GRP94) inhibitor was used to detect myocardial injury. **Results:** We found that the expression level of lncRNA-AK138945 was reduced in MIRI mouse heart tissue and H_2O_2 -treated cardiomyocytes. Moreover, the proportion of apoptosis in cardiomyocytes increased after lncRNA-AK138945 was silenced. The expression level of Bcl2 protein was decreased, and the expression level of Bad, Caspase 9 and Caspase 3 protein was increased. Our further study found that miR-1a-3p is a direct target of lncRNA-AK138945, after lncRNA-AK138945 was silenced in cardiomyocytes, the expression level of miR-1a-3p was increased while the expression level of its downstream protein GRP94 was decreased. Interestingly, treatment with a GRP94 inhibitor (PU-WS13) intensified H_2O_2 -induced cardiomyocyte apoptosis. After overexpression of FOXO3, the expression levels of lncRNA-AK138945 and GRP94 were increased, while the expression levels of miR-1a-3p were decreased. **Conclusion:** lncRNA-AK138945 inhibits GRP94 expression by regulating miR-1a-3p, leading to cardiomyocyte apoptosis. The transcription factor Forkhead Box Protein O3 (FOXO3) participates in cardiomyocyte apoptosis induced by endoplasmic reticulum stress through up-regulation of lncRNA-AK138945.

Keywords

myocardial ischemia reperfusion; lncRNA; apoptosis; microRNA GRP94

Received 08 November 2023, accepted 10 January 2024

¹State Key Laboratory of Frigid Zone Cardiovascular Diseases, and Pharmacology Department of Pharmacy college of Harbin Medical University, Harbin 150081, China

²The Fourth Department of Medical Oncology, Harbin Medical University Cancer Hospital, Harbin 150040, China

³Department of Ultrasound Imaging, the Second Affiliated Hospital of Harbin Medical University, Harbin 150086, China

⁴Cancer Institute, The Affiliated Hospital of Qingdao University, Qingdao University, Qingdao Cancer Institute, Qingdao 266071, China

⁵College of Bioinformatics Science and Technology, Harbin Medical University, Harbin 150081, China

*Corresponding authors Ying Zhang, E-mail: jennyng223@126.com; Lei Jiao, E-mail: jiaolei116@163.com; Xiaoping Leng, E-mail: xpleng@ems.hrbmu.edu.cn

*These authors contributed equally to this work

1 Introduction

Myocardial ischemia-reperfusion injury (MIRI) stands as a significant contributor to the elevated mortality rates of cardiovascular diseases (CVD). Upon its onset, MIRI not only precipitates myocardial arrhythmias but also inflicts irreversible damage upon myocardial cells, ultimately culminating in cardiac dysfunction in afflicted patients^[1-3]. Cold weather easily triggers

increases in blood pressure and heart rate, potentially leading to myocardial ischemic attacks. Numerous epidemiological studies have highlighted a strong association between low environmental temperature and increased morbidity and mortality associated with CVD^[4-7]. Regrettably, effective treatments for MIRI remain absent in clinical practice, and the underlying pathogenesis of MIRI this condition remains elusive. Consequently, the elucidation of MIRI's pathogenesis and the development of novel treatment modalities

hold paramount importance.

Long non-coding RNAs (lncRNAs) exert their regulatory influence on gene expression across various levels of the epigenetic, transcriptional, and post-transcriptional translation processes^[8]. They regulate the pathological processes of myocardial fibrosis, myocardial infarction, cardiac hypertrophy, heart failure and other. Through interactions with mRNA, DNA, proteins, and microRNAs (miRNAs), they play pivotal roles in modulating the pathological progression of major CVD, such as myocardial fibrosis, myocardial infarction, cardiac hypertrophy, and heart failure^[9-11]. Emerging evidence underscores the coordinated involvement of lncRNAs and microRNAs in the regulation of molecules implicated in cardiomyocyte apoptosis. lncRNA-MIRF has been shown to contribute to cardiomyocyte apoptosis by modulating miR-26a, subsequently promoting the expression of pro-apoptotic protein Bak1^[12]. Our previous study has revealed significant dysregulation of lncRNA-AK138945 in a mouse model of cardiac hypertrophy^[13], suggesting its potential regulatory significance in CVD. In this study, we explored the effects and underlying mechanisms through which lncRNA-AK138945 modulates MIRI.

MIRI can precipitate alterations in endoplasmic reticulum (ER) function, leading to the accumulation of unfolded or misfolded proteins and subsequently triggering endoplasmic reticulum stress (ERS). Excessive ERS stands as a pivotal factor in inducing cardiomyocyte apoptosis. Within the process of ERS, GRP94 emerges as a crucial regulator capable of degrading misfolded or unfolded proteins, thereby preserving the stability of the ER environment^[14]. Previously, we confirmed that miR-1a-3p can inhibit the expression of GRP94 by targeting its 3'UTR, consequently activating ERS to cause cardiomyocyte apoptosis^[15].

This study elucidated that lncRNA-AK138945 promoted the expression of ERS-related protein GRP94 by targeting miR-1a-3p, thereby playing a role in regulating MIRI-induced cardiomyocyte apoptosis. Therefore, supplementing exogenous or upregulating endogenous lncRNA-AK138945 might emerge as a promising therapeutic strategy for the treatment of MIRI.

2 Materials and Methods

2.1 A mouse model of myocardial ischemia-reperfusion injury

C57BL/6 mice from Liaoning Changsheng Biotechnology Co., Ltd., aged between 8 to 10 weeks and weighing between 22 g and 25 g, were selected for animal experiments. The left anterior descending (LAD) artery coronary artery of the mouse was occluded for 50 minutes using a 7-0 ligature followed by

a reperfusion period of 48 hours. (Animal Experimental Ethical Inspection Protocol No. HMUIRB3021619).

2.2 Echocardiographic analysis

Mice were intraperitoneally injected with 2, 2, 2-tribromoethanol (200 mg/kg; Sigma, St. Louis, Missouri, USA) for anesthesia, and their chests were depilated. The mice were then fixed supine on the operating table, and a proper amount of coupling agent was applied to the chest. The scanning probe was used to record the left ventricular electrocardiogram through the chest wall ultrasound and M-mode echocardiogram. Fractional shortening (FS) and ejection fraction (EF) were determined as the indicators of cardiac function.

2.3 Cell culture and cell dosing

Following the procedure described in our previous study^[16], neonatal mouse (C57BL/6) ventricular cells (NMVCs) were treated with hydrogen peroxide (100 μ mol/L, Cat#323381, Sigma-Aldrich, USA) for 48 hours to simulate MIRI *in vitro*. The NMVCs were incubated with GRP94 inhibitor PU-WS13 (5 μ mol/L; Cat#58687, MedChemExpress, USA) for 48 hours.

2.4 Construction and transfection of lncRNA siRNA and plasmid

siRNA targeting lncRNA-AK138945 (5'-GAAGAGGUAUUGAAUGCUA-3') was purchased from Ribobio (Guangzhou, Guangdong Province, China) and transfected into NMVCs following the manufacturer's instructions.

2.5 CCK8 assay

Cell counting kit-8 (CCK8, CK04-500T, Dojindo, Japan) was used to measure cell viability under different conditions. NMVCs were cultured in 96-well culture clusters (about 1×10^4 per well), followed by transfection with lncRNA-AK138945 specific siRNA for 48 hours. The CCK8 reagent (20 μ L) and DMEM (180 μ L) were added to each well and incubated for 1-4 hours. The absorbance was measured at 450 nm using an Infinite m200pro microplate spectrophotometer (Tecan, Salzburg, Austria).

2.6 Live/Dead cell staining

The cardiomyocytes were seeded on the cover glass of a 24-well culture plate. Forty-eight hours after transfection, live and dead cells were detected using the "Live/Dead Viability/Cytotoxicity Assay Kit" (Invitrogen, Shanghai, China) according to the manufacturer's instructions. A fluorescence microscope (Olympus, Tokyo, Japan) was used to acquire images.

2.7 TUNEL assay

Terminal deoxynucleotide transferase dUTP nick end labeling (TUNEL) staining was used to evaluate the apoptosis of cultured cardiomyocytes. Briefly, NMVCs cultured on coverslips in 24-well plates were fixed in 4% paraformaldehyde. TUNEL staining was conducted using the in-situ cell death detection kit (Minneapolis, MN, USA) according to the manufacturer's protocol. The numbers of TUNEL-positive cells and the total cells were counted under confocal microscopy.

2.8 Western blot

Total proteins extracted from NMVCs or mouse left ventricular tissue samples were transferred to a nitrocellulose membrane (Life Science, Überlingen, Germany) using SDS-PAGE (10%-15%). The membrane was sealed with 5% skimmed milk, and incubated overnight at 4°C with antibodies against GRP94 (Cat#20292, Cell Signaling Technology), Caspase9 (Cat#9504, Cell Signaling Technology), Caspase3 (Cat#9662, Cell Signaling Technology), Bcl2 (Cat#3498, Cell Signaling Technology), Bad (Cat#A19595, ABclonal Technology), or β -actin purchased from ZSGB-BIO (Beijing, China). Then, the membrane was washed with PBST and incubated with a secondary antibody (Alexa Fluor, Molecular Probes, Eugene, OR, USA) in the dark for 50 minutes. Odyssey v1.2 software (LI-COR Biosciences, Lincoln, NB, USA) was used to quantify the immunoblot bands. The results were normalized to the band density of β -actin.

2.9 Quantitative real-time PCR (qRT-PCR)

Total RNA was isolated from myocardial tissue and neonatal cardiomyocytes using TRIzol reagent (Invitrogen, Camarillo, CA, USA). The RNA concentration was measured by a NanoDrop 8000 spectrophotometer (Thermo Scientific, Wilmington, DE, USA). The RNA was reverse transcribed into cDNA using a reverse transcription kit (Dalian, China). Real-time quantitative PCR was performed on the Thermocycler ABI 7500 fast real-time PCR system (Applied Biosystems, Carlsbad, California, USA). The sequences of the primer pairs used in our study are:

ZFAS1-forward, 5'-AGCGTTTGCTTTGTTCCC-3', reverse5'-CTCCCTCGATGCCCTTCT-3'; AK138945-forward, 5'-AGCCCAGGAACAAATGCAGAA-3', reverse, 5'-TCAACGTCACACTTCATGATGGA-3'; CDR1as-forward, 5'-TCTGCTCGTCTTCCAACATC-3', reverse, 5'-AGATCAGCACACTGGAGAC-3'; β -ACTB-forward, 5'-ACTGCCGCATCCTCTTCCT-3'; reverse, 5'-TCAACGTCACACTTCATGATGGA-3'; miR-1a-3p-forward, 5'-GGCGTGGAATGTAAAGAA-3', reverse, 5'-CGGCAATTGCACTGGATA-3', miR-1a-3p-RT,5'-GTCGTAT

CCAGTGCGTGTCTGGAGTCGGCAATTGCACTGGATACG ACATACATAC-3'; U6-forward, 5'-GCTTCGGCAGCACATATAC TAAAT-3', reverse, 5'-CGCTTCACGAATTTGCGTGTGCAT-3', U6-RT, 5'-GCTTCGGCAGCACATATACTAAAT-3'; FOXO3-forward, 5'-CCGTGAGCAAGCCGTGTACTG-3', reverse, 5'-TATCCAGCAGGTCGTCCATGAGG-3'; GRP94-forward, 5'-ATGAAGGCACAAGCATACCAGACG-3', reverse5'-TCATCTTCCTTAATCCGCCGCAAC-3'.

2.10 Dual-luciferase reporter gene assay

HEK293T cells were transfected with miR-1a-3p mimic (20 μ mol/L), blank, miR-1a-3p inhibitor, negative control mimic (NC) or negative control inhibitor (NC inhibitor) and plasmid (0.5 μ g). Forty-eight hours after transfection, luciferase activity was measured on a fluorometer (Promega, Madison, Wisconsin, USA) using the Dual Luciferase Reporter Assay Kit (Promega, Madison, Wisconsin, USA).

2.11 Data and statistical analysis

The experimental data are expressed as mean \pm standard error (mean \pm SEM) and were statistically analyzed by one-way analysis of variance for multiple group comparisons and *t*-test for two-group comparisons (GraphPad Prism 8.0 California, United States). *P* < 0.05 was considered statistically significant.

3 Results

3.1 Downregulation of lncRNA-AK138945 in MIRI hearts and hydrogen peroxide treated cardiomyocytes

To explore the regulatory mechanisms underlying MIRI, we first established a mouse model of MIRI. Comparative analysis revealed a marked reduction in both EF and FS in the MIRI group compared to the Sham group (Fig. 1A). Moreover, the expression levels of pro-apoptotic proteins, including Caspase3, Caspase9, and Bad, were significantly increased in the MIRI group compared to the Sham group (Fig. 1B-D). Subsequently, we assessed the expression levels of circRNA-CDR1as, lncRNA-ZFAS1, and lncRNA-AK138945. We observed a substantial increase in the expression levels of circRNA-CDR1as and lncRNA-ZFAS1 in both the heart tissue of MIRI mice and H₂O₂-treated cardiomyocytes, whereas the expression level of lncRNA-AK138945 was markedly reduced (Fig. 1E and F). These findings suggest a significant decrease in the expression level of lncRNA-AK138945 during MIRI, indicating its potential regulatory role in his pathological condition.

3.2 Knockdown of lncRNA-AK138945 induces cardiomyocyte apoptosis

To further explore the impact of lncRNA-AK138945 on MIRI, we

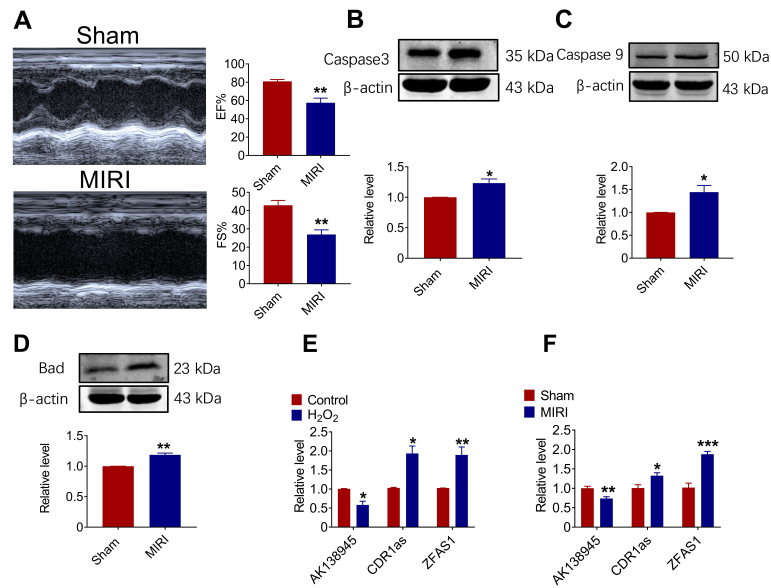


Fig. 1 Expression of lncRNA-AK138945 in a mouse model of myocardial ischemia-reperfusion injury (MIRI). (A) Significant decreases in ejection fraction (EF) and fractional shortening (FS) in MIRI mice compared to the control group, indicating the successful establishment of the MIRI model. ** vs. Sham, $P < 0.01$, Sham, $N = 6$; MIRI, $N = 4$. (B-D) Western blot analysis on the expression levels of apoptotic proteins Caspase 9, Caspase 3, and Bad in myocardial tissue. * vs. Sham, $P < 0.05$; ** vs. Sham, $P < 0.01$, $N = 3-5$. (E) qPCR analysis on the expression of lncRNA-AK138945 in neonatal mouse cardiomyocytes after hydrogen peroxide treatment. * vs. Control, $P < 0.05$; ** vs. Control, $P < 0.01$, $N = 3$. (F) Changes of lncRNA-AK138945 expression in cardiac tissue of MIRI model. * vs. Sham, $P < 0.05$; ** vs. Sham, $P < 0.01$; *** vs. Sham, $P < 0.001$, $N = 3-4$.

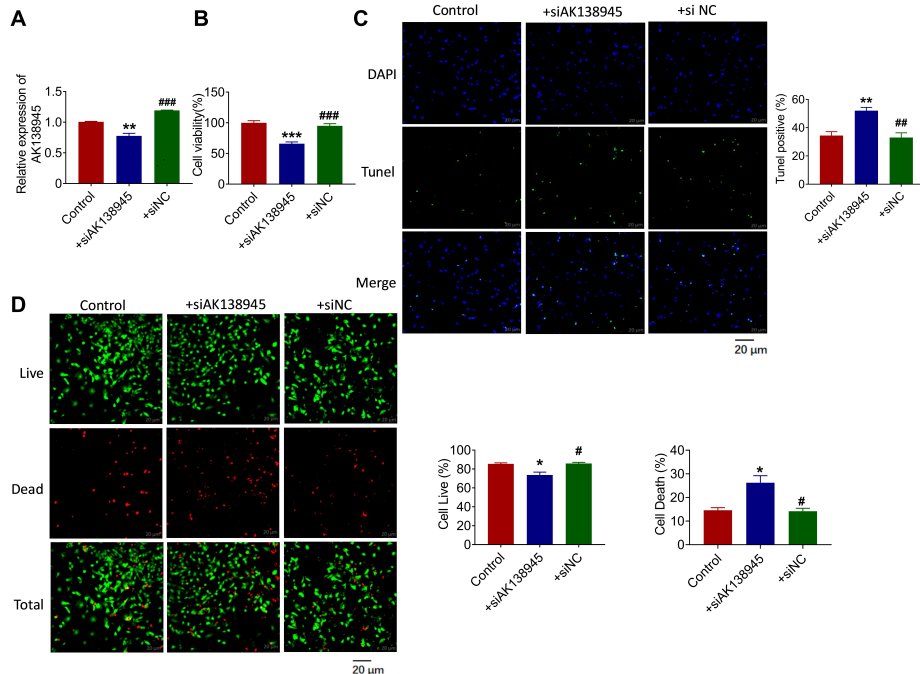


Fig. 2 lncRNA-AK138945 knockdown facilitates cardiomyocyte apoptosis. (A) Verification of lncRNA-AK138945 knockdown efficiency by its siRNA (siAK138945) ** vs. Control, $P < 0.01$; *** vs. +siAK138945, $P < 0.001$, $N = 3$. (B) Reduced cardiomyocyte viability by siAK138945, as measured by CCK8 assay. *** vs. Control, $P < 0.001$; *** vs. +siAK138945, $P < 0.001$, $N = 6$. (C) siAK138945 increased cardiomyocyte apoptosis by siAK138945 as unveiled by TUNEL staining. ** vs. Control, $P < 0.01$; # vs. +siAK138945, $P < 0.01$, $N = 3$. (D) siAK138945 increased cardiomyocyte death, as demonstrated by survival/death (Live/Dead) staining. Red fluorescence represents dead cells, and green fluorescence represents live cells. * vs. Control, $P < 0.05$; # vs. +siAK138945, $P < 0.05$, $N = 3$.

designed and validated a siRNA targeting lncRNA-AK138945 (siAK138945) and confirmed its efficiency in knockdown (Fig. 2A). Comparative analysis revealed a noticeable reduction in cell viability following the knockdown of lncRNA-AK138945 relative to the control group (Fig. 2B). Moreover, silencing lncRNA-AK138945 increased the ratio of TUNEL-positive cells (Fig. 2C), indicating apoptotic cell death. This was further evidenced by the increased cell death rate in siAK138945-treated cardiomyocytes, as revealed by Live/Dead cell staining experiments (Fig. 2D). These findings indicate that knockdown of lncRNA-AK138945 can induce cardiomyocyte apoptosis. To corroborate this inference mechanistically, we examined the effects of lncRNA-AK138945 on apoptosis-related proteins in cardiomyocytes. Noticeably, lncRNA-AK138945 knockdown elevated the levels of pro-apoptotic proteins like Bad, Caspase9, and Caspase3 and reduced the expression of anti-apoptotic protein Bcl-2 (Fig. 3A-D). These data collectively indicate that decreased expression of lncRNA-AK138945 may contribute to MIRI *via* regulating myocardial cell apoptosis.

3.3 MiR-1a-3p is a direct target of lncRNA-AK138945

Subsequently, we endeavored to elucidate why the decreased expression of lncRNA-AK138945 induces myocardial damage. To this end, we conducted an analysis and prediction of microRNAs that can potentially be regulated by lncRNA-AK138945 using a bioinformatics database (<http://bibiserv.techfak.uni-bielefeld.de/rnahybrid>). Our analysis revealed that lncRNA-AK138945 has the potential to interact with miR-1a-3p, as depicted in Fig. 4A. To confirm the direct interaction between lncRNA-AK138945 and miR-1a-3p, we both cloned the wild-type and mutant miR-1a-3p containing the binding site for lncRNA-AK138945 into a luciferase reporter vector. Then, we co-transfected these constructs with miR-1a-3p, blank, miR-1a-3p inhibitor, NC, and NC inhibitor into HEK293T cells and evaluated the effects of miR-1a-3p on luciferase activity. Comparative analysis revealed a significant reduction in the luciferase activity of lncRNA-AK138945 in the miR-1a-3p group compared to the NC group, and this reduction was restored after mutation of the binding site (Fig. 4B). Moreover, we observed a significant increase in the level of miR-1a-3p following lncRNA-AK138945 knockdown (Fig. 4C). These results collectively indicate that miR-1a-3p is a direct target of lncRNA-AK138945.

We next proceeded to uncover the underlying downstream molecular mechanism of lncRNA-AK138945. Our previous study had already identified miR-1a-3p as a key regulator of MIRI by targeting GRP94^[15]. Therefore, we further explored the regulatory relationship between lncRNA-AK138945 and GRP94. As depicted in Fig. 4D and Fig. 4E, lncRNA-AK138945 knockdown markedly reduced the expression of GRP94 at both mRNA and protein

levels compared to the siNC group. These findings strongly suggest the existence of the lncRNA-AK138945-miR-1a-3p-GRP94 regulatory pathway during MIRI.

3.4 Inhibition of GRP94 induces myocardial cell apoptosis.

GRP94 serves as a type of molecular chaperone, actively participating in the ER quality control system and regulating the ER stress signaling pathway. Following myocardial ischemia-reperfusion, there is a notable increase in GRP94 levels^[17]. To further investigate the relationship between GRP94 and apoptosis during MIRI, we utilized PU-WS13, a potent GRP94-specific Hsp90 inhibitor with purine scaffolds^[18], in our experiments. Upon administration of PU-WS13, there was a significant increase in the expression levels of pro-apoptotic proteins in the H₂O₂-treated cardiomyocytes, accompanied by a decrease in the expression level of anti-apoptotic proteins (Fig. 5A-D).

3.5 Effect of transcription factor FOXO3 on the AK138945-miR-1-GRP94 signaling pathway

To further elucidate the upstream mechanism of lncRNA-AK138945 in regulating MIRI, we used the JASPAR database (<http://jaspar.genereg.net/>) to predict the potential transcription factors of lncRNA-AK138945. As illustrated in Supplementary Material 1, we identified 12 potential FOXO3 recognition/binding sites in the lncRNA-AK138945 sequence, suggesting that FOXO3 may play a role in regulating the lncRNA-AK138945-miR-1-GRP94 signaling pathway. It has been reported that FOXO3 deficiency can lead to increased oxidative damage and decreased myocardial function following acute ischemia-reperfusion injury^[19]. Furthermore, our analysis revealed a significant reduction in the expression of FOXO3 during MIRI, further corroborating these findings (Fig. 6A). Subsequently, we constructed a FOXO3 overexpression plasmid and confirmed its efficiency (Fig. 6B). Notably, FOXO3 overexpression significantly increased the expression levels of lncRNA-AK138945 and GRP94, while inhibiting the expression of miR-1a-3p (Fig. 6C-E). This finding suggests that FOXO3 exerts a regulatory effect on the lncRNA-AK138945-miR-1-GRP94 signaling pathway.

4 Discussion

Abnormal expression of lncRNA plays a crucial role in CVD, drawing significant attention in recent years due to their regulatory roles in various physiological and pathological processes. Previous studies have documented the involvement of specific lncRNAs in cardiomyocyte apoptosis and MIRI. For instance, lncRNA-6395, recognized as an endogenous proapoptotic factor, regulates cardiomyocyte apoptosis and MIRI by inhibiting the

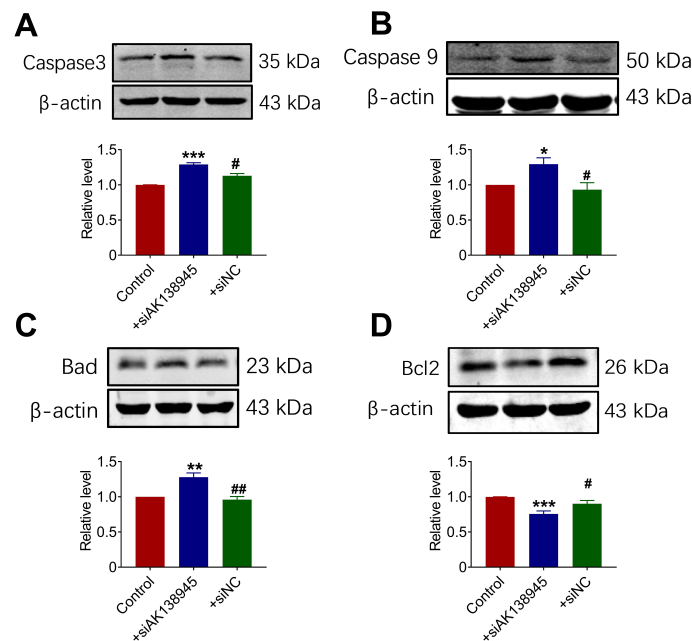


Fig. 3 LncRNA-AK138945 knockdown anomaly alters the expression of apoptosis-related proteins in cardiomyocytes. (A-C) LncRNA-AK138945 knockdown by siAK138945 increases the expression levels of apoptotic proteins Caspase3, Caspase9, and Bad in cardiomyocytes. * vs. Control, $P < 0.05$; ** vs. Control, $P < 0.01$; *** vs. Control, $P < 0.001$; # vs. +siAK138945, $P < 0.05$; ## vs. +siAK138945, $P < 0.01$, $N = 3-4$. (D) siAK138945 significantly reduced the expression of Bcl2. *** vs. Control, $P < 0.001$; # vs. +siAK138945, $P < 0.05$, $N = 5$.

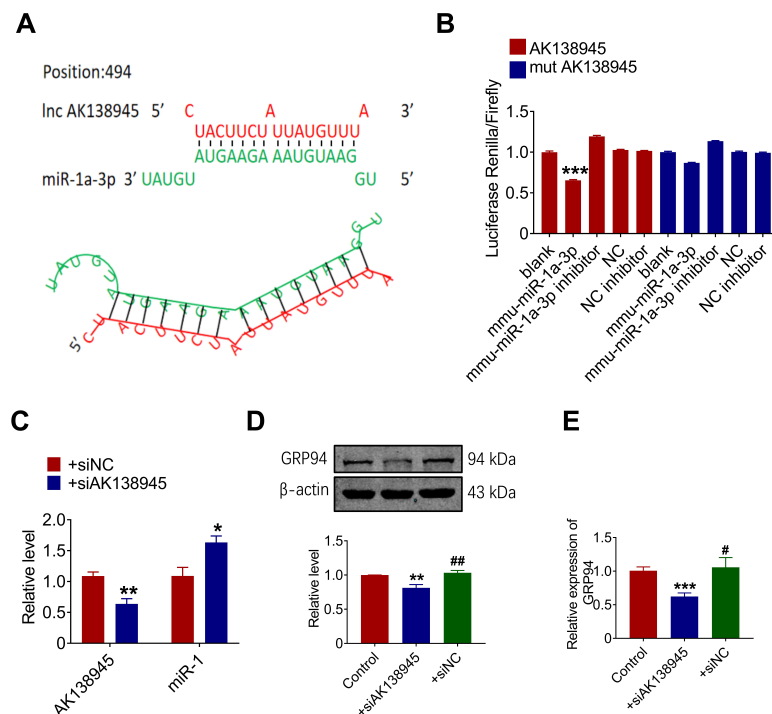


Fig. 4 Experimental verification of miR-1a-3p as a downstream target of LncRNA-AK138945. (A) The predicted binding sites between miR-1a-3p and LncRNA-AK138945. (B) Luciferase reporter gene activity. *** vs. NC, $P < 0.001$, $N = 3$. (C) Upregulation of miR-1a-3p expression following LncRNA-AK138945 knockdown. * vs. +siNC, $P < 0.05$; ** vs. +siNC, $P < 0.01$, $N = 3-6$. (D-E) Downregulation of GRP94 expression post-LncRNA-AK138945 knockdown. ** vs. Control, $P < 0.01$; *** vs. Control, $P < 0.001$; # vs. +siAK138945, $P < 0.05$; ## vs. +siAK138945, $P < 0.01$, $N = 5-6$.

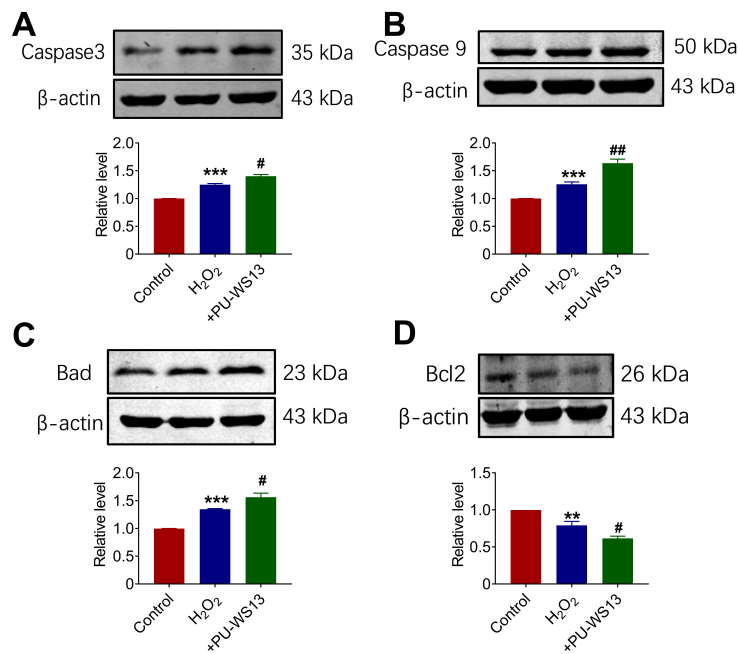


Fig. 5 Inhibition of GRP94 induces cardiomyocyte apoptosis. (A-C) After treatment with a GRP94 inhibitor, the expression of apoptosis-related proteins Caspase3, Caspase9 and Bad was increased. *** vs. Control, $P < 0.001$; # vs. H_2O_2 , $P < 0.05$, ## vs. H_2O_2 , $P < 0.01$, $N = 3-6$. (D) The expression of anti-apoptotic protein Bcl2 was reduced after treatment with GRP94 inhibitor. ** vs. Control, $P < 0.01$; # vs. H_2O_2 , $P < 0.05$, $N = 6$.

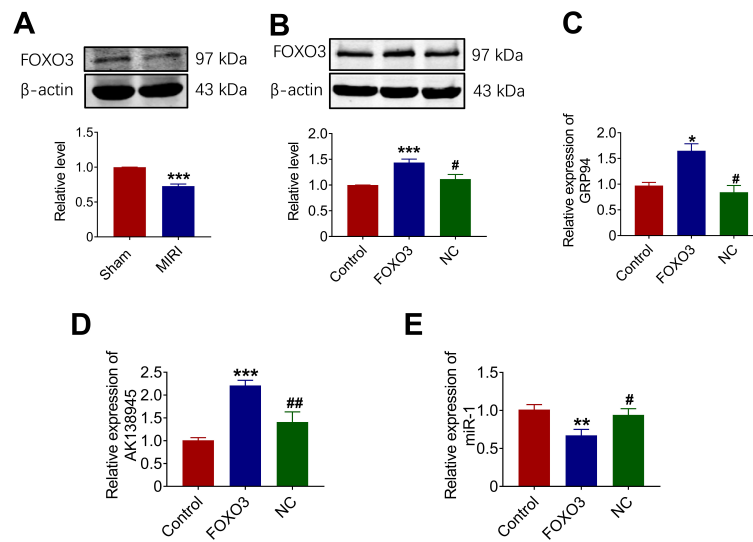


Fig. 6 Effect of transcription factor FOXO3 on the AK138945-miR-1-GRP94 signaling pathway. (A) The expression of FOXO3 in myocardial tissue. *** vs. Sham, $P < 0.001$, Sham, $N = 4$; MIRI, $N = 4$. (B) Verification of FOXO3 overexpression efficiency. *** vs. Control, $P < 0.001$; # vs. FOXO3, $P < 0.05$, $N = 4$. (C-D) The expression levels of lncRNA-AK138945 and GRP94 are up-regulated after FOXO3 overexpression. * vs. Control, $P < 0.05$; *** vs. Control, $P < 0.001$; # vs. FOXO3, $P < 0.05$; ## vs. FOXO3, $P < 0.01$, $N = 6$. (E) FOXO3 overexpression downregulates the expression level of miR-1a-3p. ** vs. Control, $P < 0.01$; # vs. FOXO3, $P < 0.05$, $N = 6$.

degradation of p53 and promoting its subcellular translocation^[20]. Additionally, our group has identified ZFAS1 as elevated during MIRI, attributing to its role in myocardial injury by increasing oxidative stress and cell apoptosis^[21]. Furthermore, lncRNA-

AK138945 was found to be significantly dysregulated in a mouse model of cardiac hypertrophy in a previous study^[11]. In our current work, we took the pioneering step to speculate on its function in MIRI. Surprisingly, findings revealed a marked decrease in

Certificate of China Postdoctoral Science Foundation Grant (2021M693826), the postdoctoral funding from Heilongjiang Province (21042230046) and the Hai Yan Youth Fund from Harbin Medical University Cancer Hospital (JJQN2021-09).

Ethics approval

The use of animals was approved by the Ethics Committee of Harbin Medical University and complies with the Guidelines for the Care and Use of Laboratory Animals published by the National

Institutes of Health.

Conflict of interest

The author declares that there is no conflict of interest.

Data availability statement

The data are presented in the study and further inquiries can be directed to the corresponding author.

References

- [1] Clark D P, Hanke C W, Swanson N A. Dermal implants: safety of products injected for soft tissue augmentation. *J Am Acad Dermatol*, 1989(5 Pt 1); 21: 992-998.
- [2] Inoue T. Ischemia-reperfusion injury is still a big hurdle to overcome for treatment of acute myocardial infarction. *J Cardiol*, 2016; 67(4): 305-306.
- [3] Poss J, Desch S, Eitel C, *et al*. Left ventricular thrombus formation after st-segment-elevation myocardial infarction: insights from a cardiac magnetic resonance multicenter study. *Circ Cardiovasc Imaging*, 2015; 8(10): e003417.
- [4] Lv L S, Zhou C L, Jin D H, *et al*. Impact of ambient temperature on life loss per death from cardiovascular diseases: a multicenter study in central China. *Environ Sci Pollut Res Int*, 2022; 29(11): 15791-15799.
- [5] Fonseca-Rodriguez O, Sheridan S C, Lundevaller E H, *et al*. Effect of extreme hot and cold weather on cause-specific hospitalizations in Sweden: A time series analysis. *Environ Res*, 2021; 193: 110535
- [6] Hu J, Hou Z, Xu Y, *et al*. Life loss of cardiovascular diseases per death attributable to ambient temperature: A national time series analysis based on 364 locations in China. *Sci Total Environ*, 2021; 756: 142614.
- [7] Xu E, Li Y N, Li T T, *et al*. Association between ambient temperature and ambulance dispatch: a systematic review and meta-analysis. *Environ Sci Pollut Res Int*, 2022; 29(44): 66335-66347.
- [8] Heo J B, Lee Y S, Sung S. Epigenetic regulation by long noncoding RNAs in plants. *Chromosome Res*, 2013; 21(6-7): 685-693.
- [9] Zhang Y, Jiao L, Sun L, *et al*. Lncrna Zfas1 as a Serca2a inhibitor to cause intracellular Ca(2+) overload and contractile dysfunction in a mouse model of myocardial infarction. *Circ Res*, 2018; 122(10): 1354-1368.
- [10] Sun F, Zhuang Y, Zhu H, *et al*. Lncrna Pcf1 promotes cardiac fibrosis via mir-378/Grb2 pathway following myocardial infarction. *J Mol Cell Cardiol*, 2019; 133: 188-198.
- [11] Cai B, Zhang Y, Zhao Y, *et al*. Long noncoding RNA-DACH1 (dachshund homolog 1) regulates cardiac function by inhibiting SERCA2a (sarcoplasmic reticulum calciumATPase 2a). *Hypertension*, 2019; 74(4): 833-842.
- [12] Su X, Lv L, Li Y, *et al*. Lncrna Mirf promotes cardiac apoptosis through the miR-26a-Bak1 axis. *Mol Ther Nucleic Acids*, 2020; 20: 841-850.
- [13] Sun L, Zhang Y, Zhuang Y, *et al*. Expression profile of long non-coding RNAs in a mouse model of cardiac hypertrophy. *Int J Cardiol*, 2014; 177(1): 73-75.
- [14] Fonseca S G, Urano F, Burcin M, *et al*. Stress hyperactivation in the beta-cell. *Islets*, 2010; 2: 1-9.
- [15] Zhang Y, Liu X, Zhang L, *et al*. Metformin protects against H₂O₂-induced cardiomyocyte injury by inhibiting the miR-1a-3p/GRP94 pathway. *Mol Ther Nucleic Acids*, 2018; 13: 189-197.
- [16] Liu X, Zhang Y, Du W, *et al*. MiR-223-3p as a novel microRNA regulator of expression of voltage-gated K⁺ channel Kv4.2 in acute myocardial infarction. *Cell Physiol Biochem*, 2016; 39(1): 102-114.
- [17] Martindale J J, Fernandez R, Thuerlauf D, *et al*. Endoplasmic reticulum stress gene induction and protection from ischemia/reperfusion injury in the hearts of transgenic mice with a tamoxifen-regulated form of ATF6. *Circ Res*, 2006; 98(9): 1186-1193.
- [18] Tramentozzi E, Finotti P. Effects of purine-scaffold inhibitors on HUVECs: involvement of the purinergic pathway and interference with ATP. Implications for preventing the adverse effects of extracellular GRP94. *Biochem Biophys Rep*, 2019; 19: 100661.
- [19] Sengupta A, Molkentin J D, Paik J H, *et al*. Foxo transcription factors promote cardiomyocyte survival upon induction of oxidative stress. *J Biol Chem*, 2011; 286(9): 7468-7478.
- [20] Zhan L F, Zhang Q, Zhao L, *et al*. LncRNA-6395 promotes myocardial ischemia-reperfusion injury in mice through increasing p53 pathway. *Acta Pharmacol Sin*, 2022; 43(6): 1383-1394.
- [21] Li M, Jiao L, Shao Y, *et al*. LncRNA-ZFAS1 promotes myocardial ischemia-reperfusion injury through DNA methylation-mediated Notch1 down-regulation in mice. *JACC Basic Transl Sci*, 2022; 7(9): 880-895.
- [22] Ebner A, Poitz D M, Alexiou K, *et al*. Secretion of adiponectin from mouse aorta and its role in cold storage-induced vascular dysfunction. *Basic Res Cardiol*, 2013; 108(6): 390
- [23] Xue Y, Yu X, Zhang X, *et al*. Protective effects of ginsenoside Rc against acute cold exposure-induced myocardial injury in rats. *J Food Sci*, 2021; 86(7): 3252-3264.
- [24] Cong P, Liu Y, Liu N, *et al*. Cold exposure induced oxidative stress and apoptosis in the myocardium by inhibiting the Nrf2-Keap1 signaling pathway. *BMC Cardiovasc Disord*, 2018; 18(1): 36.
- [25] Park J, Kim S, Kim D H, *et al*. Whole-body cold tolerance in older Korean female divers "haenyeo" during cold air exposure: effects of repetitive cold exposure and aging. *Int J Biometeorol*, 2018; 62(4): 543-551.
- [26] Yin Z Q, Ding G B, Chen X, *et al*. Beclin1 haploinsufficiency rescues

low ambient temperature-induced cardiac remodeling and contractile dysfunction through inhibition of ferroptosis and mitochondrial injury. *Metabolism*, 2020; 113: 154397.

[27] Jiang S, Guo R, Zhang Y, *et al.* Heavy metal scavenger metallothionein mitigates deep hypothermia-induced myocardial contractile anomalies: role of autophagy. *Am J Physiol Endocrinol Metab*, 2013; 304(1): E74-86.

[28] Zhang Y, Li L, Hua Y, *et al.* Cardiac-specific knockout of ET(A) receptor mitigates low ambient temperature-induced cardiac hypertrophy and contractile dysfunction. *J Mol Cell Biol*, 2012; 4(2): 97-107.

[29] Zhang Y M, Hu N, Hua Y A, *et al.* Cardiac over expression of metallothionein rescues cold exposure-induced myocardial contractile dysfunction through attenuation of cardiac fibrosis despite cardiomyocyte mechanical anomalies. *Free Radic Biol Med*, 2012; 53(2): 194-207.

[30] Liang J, Yin K, Cao X, *et al.* Attenuation of low ambient temperature-induced myocardial hypertrophy by atorvastatin *via* promoting Bcl-2 expression. *Cell Physiol Biochem*, 2017; 41(1): 286-295.

[31] Yin K, Zhao L, Feng D, *et al.* Resveratrol attenuated low ambient temperature-induced myocardial hypertrophy *via* inhibiting cardiomyocyte apoptosis. *Cell Physiol Biochem*, 2015; 35(6): 2451-2462.

[32] Ebner A, Poitz D M, Alexiou K, *et al.* Secretion of adiponectin from mouse aorta and its role in cold storage-induced vascular dysfunction. *Basic Res Cardiol*, 2013; 108(6): 390.

[33] Chen T, Gu Y, Bai G H, *et al.* MiR-1a-3p Inhibits apoptosis in fluoride-exposed LS8 cells by targeting Map3k1. *Biol Trace Elem Res*, 2023.

[34] He R, Ding C, Yin P, *et al.* MiR-1a-3p mitigates isoproterenol-induced heart failure by enhancing the expression of mitochondrial ND1 and COX1. *Exp Cell Res*, 2019; 378(1): 87-97.